

STEEL FIBRE REINFORCED HIGH PERFORMANCE CONCRETE BEAM-COLUMN JOINTS SUBJECTED TO CYCLIC LOADING

N. Ganesan, P.V. Indira and Ruby Abraham

Department of Civil Engineering
National Institute of Technology
Calicut-673601

ABSTRACT

This paper describes the experimental results of ten steel fibre reinforced high performance concrete (SFRHPC) exterior beam-column joints under cyclic loading. The M60 grade concrete used was designed by using a modified ACI method suggested by Aïtcin. Volume fraction of the fibres used in this study varied from 0 to 1% with an increment of 0.25%. Joints were tested under positive cyclic loading, and the results were evaluated with respect to strength, ductility and stiffness degradation. Test results indicate that the provision of SFRHPC in beam-column joints enhances the strength, ductility and stiffness, and is one of the possible alternative solutions for reducing the congestion of transverse reinforcement in beam-column joints. Also, an attempt has been made to compare the shear strengths of beam-column joints obtained by using the models proposed by Tsonos and co-workers, Bakir and co-workers, and Jiuru and co-workers. As these models are meant for the joints in ordinary concrete, comparison was not found to be satisfactory. The model proposed by Jiuru and co-workers was modified to account for the presence of high performance concrete. The proposed model was found to compare satisfactorily with the test results.

KEYWORDS: Beam-Column Joint, High Performance Concrete, Steel Fibres, Strength, Ductility

INTRODUCTION

Recent earthquakes in different parts of the world have revealed again the importance of design of reinforced concrete structures with high ductility. Strength and ductility of structures depend mainly on proper detailing of the reinforcement in beam-column joints. The flow of forces within a beam-column joint may be interrupted if the shear strength of the joint is not adequately provided. Under seismic excitations, the beam-column joint region is subjected to horizontal and vertical shear forces whose magnitudes are many times higher than those within the adjacent beams and columns. Conventional concrete loses its tensile resistance after the formation of multiple cracks. However, fiber concrete can sustain a portion of its resistance following cracking to resist more cycles of loading. Beam-column joints have a crucial role in the structural integrity of the buildings. For this reason they must be provided with adequate stiffness and strength to sustain the loads transmitted from beam and columns. The formation of plastic hinges in columns must be prevented since it affects the entire structure. For adequate ductility of beam-column joints, use of closely spaced hoops as transverse reinforcement was recommended in the ACI-ASCE Committee 352 report (ACI, 2002). Due to the congestion of reinforcement, casting of beam-column joint will be difficult and will lead to honeycombing in concrete (Kumar et al., 1991).

Review of literature indicates that numerous studies were conducted in the past to study the behaviour of beam-column joints with normal concrete (Shamim and Kumar, 1999; Gefken and Ramey, 1989; Filiatrault et al., 1994; Soubra et al., 1993; Tsonos et al., 1992). ACI-ASCE Committee 352 makes recommendations on the design aspects of different types of beam-column joints, calculation of shear strength, and on reinforcement details to be provided (ACI, 2002). However, those recommendations are not intended for the fibre reinforced concrete. Bakir (2003) has carried out extensive research on parameters that influence the behaviour of cyclically loaded joints, and has derived equations for calculating the shear strength of the joints. A study conducted on fibre reinforced normal strength concrete by Filiatrault et al. (1994) indicates that this material is an alternative to the confining reinforcement in the joint region. The result of the study conducted by Gefken and Ramey (1989) shows that joint hoop spacing specified by ACI-ASCE Committee can be increased by a factor of 1.7 by the addition of fibres in a mix. Jiuru et al. (1992) also have studied the effect of fibres on the beam-column joint and have developed equations for predicting the shear strength of joints for normal strength concrete.

Bayasi and Gebman (2002) also experimentally proved the confinement effect of fibres in the joint region and a reduction in the lateral reinforcement by the use of fibre concrete.

Besides these, there are a large number of investigations on the effect of addition of fibres on the strength and ductility of flexural members. The study carried out by Oh (1992) indicates that ductility and ultimate resistance of flexural members are remarkably enhanced due to the addition of steel fibres. Also it was emphasised that the neglect of fibre contribution may considerably underestimate the flexural capacity of fibre reinforced concrete beams. However, the investigation carried out by Espion (1994) contradicts the findings of Oh (1992). As reported by ACI Committee 544 based on a large number of investigations, there is a considerable improvement in strength, ductility, and energy absorption capacity with the addition of steel fibres (ACI, 1988). All these studies are limited to the normal strength concrete, and the research in the area of high performance concrete (HPC) and steel fibre reinforced high performance concrete (SFRHPC) beam-column joints is limited. In general, when fibres are added to concrete, tensile strain in the neighbourhood of fibres improves significantly. In the case of SFRHPC, since concrete is dense even at the microstructure level, tensile strain would be much higher than that of the conventional SFRC. This, in turn, will improve the cracking behaviour, ductility and energy absorption capacity of the composite. This is in addition to the durability aspect of plain HPC. In order to tap the potential of SFRHPC, the existing body of knowledge must be expanded. Hence, an attempt has been made to study the behaviour of SFRHPC beam-column joint under the positive cyclic loading.

EXPERIMENTAL PROGRAMME

1. Mix Proportions

HPC mix proportions for M60 grade concrete were obtained based on the ACI 211 guidelines (ACI, 1998), as modified by Aïtcin (Aïtcin, 1998). The details of mix proportions thus obtained are given in Table 1. Part of the cement was replaced by micro-fillers such as silica fume and fly ash. In this study 10% replacement of cement by silica fume and 20% by fly ash was considered. Workability of the mix was kept constant at the compaction factor of 0.9. Same mix proportions were maintained for all the mixes. However, as the steel fibres were added to the HPC, the workability was found to decrease. Hence in order to maintain uniform workability, dosage of superplasticizer was adjusted in the SFRHPC mix.

Table 1: HPC Mix Proportions (kg/m³)

Cement	Fly ash	Silica fume	Sand	Coarse aggregate	Water	Superplasticizer
353	98	39	658	1048	162	10.78

2. Specimen Details

In the present investigation, ten exterior beam-column joints were cast and tested under flexural cyclic loading. The overall dimensions and the details of the reinforcement of the beam-column joints are given in Figure 1. The column was reinforced with four 12 mm diameter high yield strength deformed (HYSD) bars, and the beam was provided with two 12 mm diameter HYSD bars at the top and bottom. HYSD bars of 6 mm diameter were used for transverse ties in the columns and stirrups in the beams. Four different volume fractions of fibres, viz., 0.25, 0.50, 0.75, and 1.00, were used for the SFRHPC mix. At the volume fractions of fibres (v_f) above 1%, concrete mix became less workable, and hence, only the mixes up to $v_f = 1\%$ were considered in this study. Details of the specimens tested are given in Table 2.

3. Casting of Specimens

3.1 Materials Used

Ordinary Portland Cement (53 grade) conforming to IS: 8112-1989 (BIS, 1989) was used for the investigation along with the silica fume supplied by ELKEM micro silica and fly ash supplied by Neyveli Lignite Corporation. The fine aggregate used was river sand passing through 4.75 mm IS sieve and having a fineness modulus of 2.46. Crushed granite stones passing 12.5 mm and retained on 4.75 mm and

having a fineness modulus of 6.89 were used. Crimped steel fibres with an aspect ratio of 66 were used throughout the study. A naphthalene-based superplasticizer was added to the mixes for getting required workability.

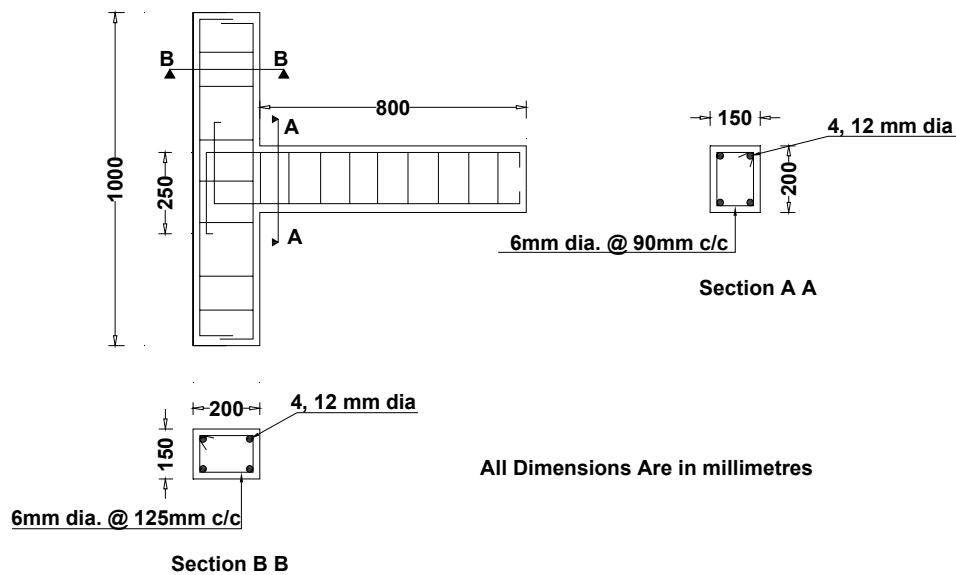


Fig. 1 Reinforcement details

Table 2: Details of Specimens and Test Results

Specimen No.	ν_f (%)	f'_c (N/mm ²)	First Crack Load P_{cr} (kN)	Ultimate Load P_u (kN)	Deflection δ_u at Peak Load (mm)	Curvature at Ultimate Load $\Phi_u \times 10^{-3}$ (rad/m)	Curvature Ductility Factor Φ_u / Φ_y
HP _r	0.00	76.20	9.32	23.54	29.00	40.30	2.80
F1HP _r	0.25	77.70	9.81	25.51	32.44	45.30	3.15
F2HP _r	0.50	79.00	10.29	26.48	36.00	47.50	3.30
F3HP _r	0.75	79.20	10.79	29.43	42.17	53.70	3.75
F4HP _r	1.00	81.00	11.28	32.37	51.00	59.00	4.04

3.2 Casting

Steel moulds were used for casting the specimens. Reinforcement cages were fabricated and placed inside the moulds. Required quantities of cement, sand and coarse aggregate were mixed thoroughly in a drum type mixer machine, and 50% of water was added to the dry mix. The remaining 50% water, mixed with the superplasticizer, was added later along with the mineral admixtures silica fume and fly ash. Mixing was done till a uniform mix was obtained. The mixes were poured into moulds in layers, and the moulds were vibrated for thorough compaction. Immediately after casting, specimens were covered with wet gunny bags to prevent loss of moisture. After 24 hours, specimens were demoulded and cured under wet gunny bags for 28 days.

3.3 Testing of Specimens

Specimens were tested in a universal testing machine of 294.3 kN (or 30 t) capacity. A constant load of 15.7 kN (or 1.6 t), which is about 20% of the axial capacity of the column, was applied to the columns for holding the specimens in position and to simulate column axial load. A hydraulic jack of 4.9 kN (or 0.5 t) capacity was used to apply load at the beam as shown in Figure 2. A load cell of 4.9 kN (or 0.5 t) capacity was used to measure the applied load accurately. A dial gauge with a least count of 0.01 mm was

used to measure the beam tip displacements. The increment of loading was taken as 0.5 kN. The beam was loaded up to the first increment, then unloaded and reloaded to the next increment of load, and this pattern of loading was continued for each increment. Three numbers of linear variable differential transducers (LVDTs) were used to measure the deformations, and later strains, at different locations. The gauge length of each LVDT was 200 mm. One LVDT was used to verify whether there is any axial deformation, and the other two LVDTs were used to measure the beam rotations. The locations of the LVDTs are shown in Figure 2, and the photograph of the test setup is shown in Figure 3.

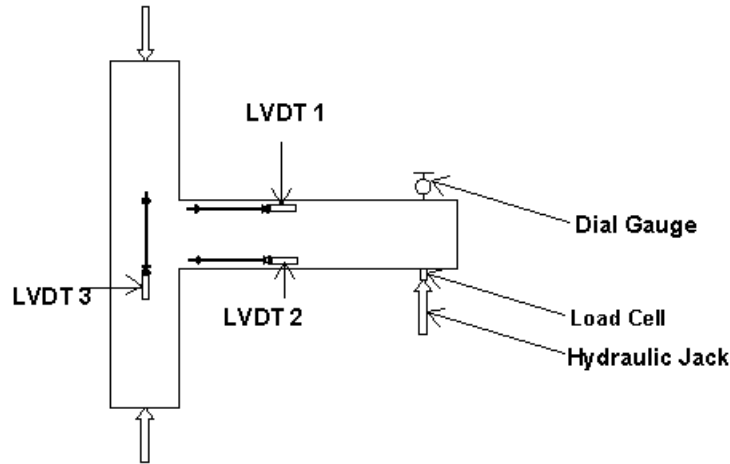


Fig. 2 Locations of LVDTs on the beam-column joint



Fig. 3 Test setup

BEHAVIOUR OF SPECIMENS

In all specimens, cracks appeared near the joint after the first crack load. With further increase in loading, the cracks propagated up the beam and initial cracks started widening. A large number of closely spaced finer cracks appeared in the SFRHPC beam-column joint specimens, and the width of such cracks was smaller than the crack-width in the HPC beam-column joint specimens. The ultimate load and corresponding deflection of specimens were found to increase as the fibre content increased. The typical failure patterns of HPC and SFRHPC beam-column joints are shown in Figures 4(a) and 4(b), respectively.

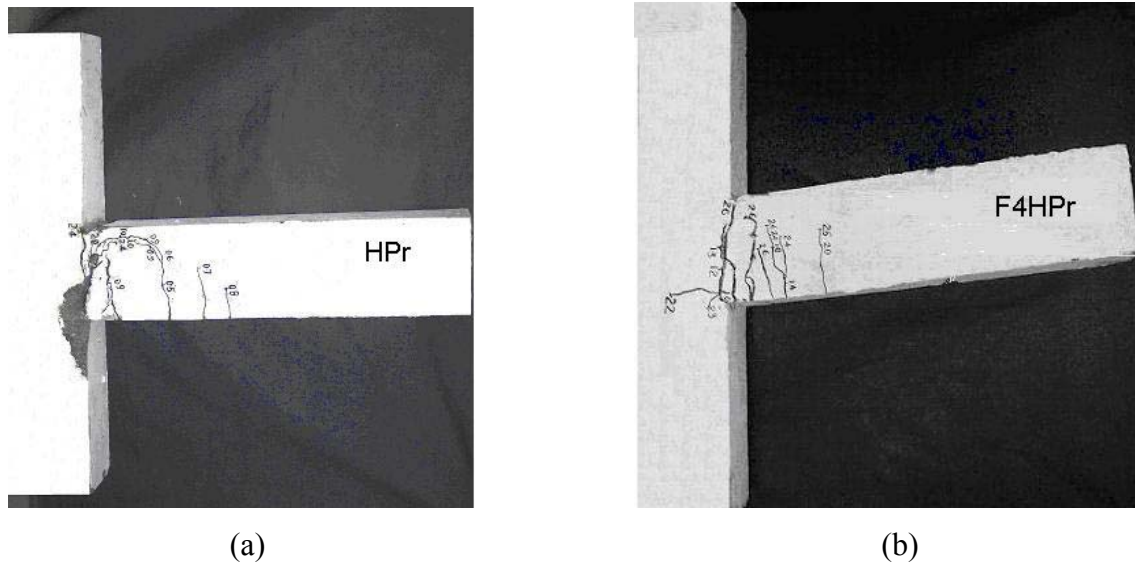


Fig. 4 (a) HPC specimen after failure; (b) SFRHPC specimen after failure

RESULTS AND DISCUSSION

1. Ultimate Load

For each value of v_f two specimens were tested. As the difference between the two test results was found to be less than 15%, the average values of the test results are taken and are given in Table 2. Results show an increase of about 20% in the first crack load and 37% in the ultimate load for the SFRHPC specimens with 1% steel fibres. The increase in ultimate load may be due to the following reasons. As and when the micro-cracks develop in the matrix, fibres intercept the cracks and prevent them from propagating in the same direction (Ganesan and Indira, 2000). Hence the cracks have to take a deviated path, which requires more energy for further propagation, thus resulting in higher load carrying capacity. During cyclic loading, when unloading takes place, tip of the crack becomes blunt, and during reloading the specimen, more energy is required to propagate the crack or to change the direction of propagation from the blunt crack tip. This in turn increases the ultimate load.

2. Load-Deflection Behaviour

A typical load-deflection plot is shown in Figure 5. The envelope curve is obtained by joining the peak points of each cycle. A comparison of the envelope plots for different volume fractions of fibres is given in Figure 6. Referring to Figure 6, it can be seen that HPC specimens with fibres showed, more or less, no strength degradation for the descending portion of the load-deflection plot and that the load carrying capacity of the joints increased with increasing fibre content. The area under the load-deflection curve represents the energy absorption capacity of the specimen. The results also show an increase of about 75% in deflection at the ultimate load for the specimens with 1% fibres.

3. Curvature Ductility Factor

The performance of a beam-column joint can be characterized by curvature ductility factor, defined as the ratio of the curvature at the peak load to the curvature at the yielding of reinforcement. The curvature at yield can be calculated as

$$\phi_y = \frac{f_y}{E_s (d - x)} \tag{1}$$

The values of f_y and E_s were experimentally determined, and the curvature ductility factor was obtained by using Equation (1) for all the specimens. It can be seen from Table 2 that as the volume fraction of

fibres increased, the curvature ductility factor was also found to increase and that it is about 145% higher in the case of specimens with fibres having $v_f = 1\%$ as compared to the HPC specimens.

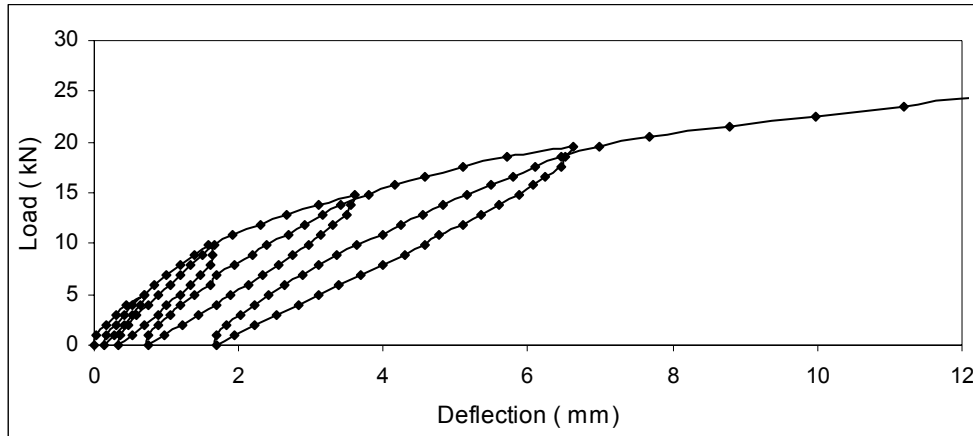


Fig. 5 Typical load-deflection plot

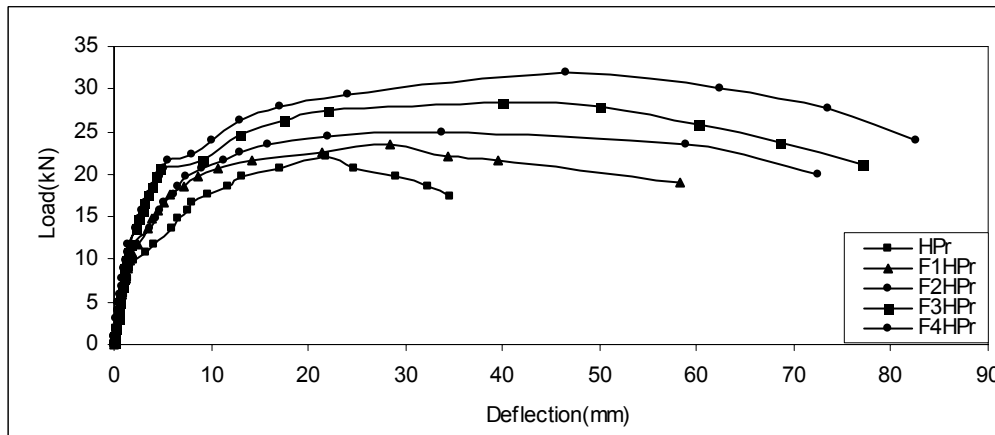


Fig. 6 Comparison of the envelope curves

4. Stiffness Degradation

In the case of reinforced concrete beam-column joints, stiffness of the joint gets reduced when the joint is subjected to cyclic/repeated/dynamic loading. This reduction in stiffness is due to the following reasons.

During cyclic loading, the materials, viz. concrete and steel, are subjected to loading, unloading, and reloading processes. This will cause initiation of micro-cracks inside the joint and will sometimes lead to the fatigue limit of the materials. This, in turn, increases the deformations inside the joints, thus resulting in reduction in the stiffness. Hence, it is necessary to evaluate degradation of stiffness in the beam-column joints subjected to cyclic or repeated loading. In order to determine the degradation of stiffness, the following procedure was adopted.

A line 0-1 joining the origin and the peak load of the first cycle, as shown in Figure 7, is drawn. The slope of this line is known as the secant stiffness (Shannag et al., 2005). Similarly, from the slope of the line joining the points 2 and 3 of the second cycle, secant stiffness of the second cycle is obtained. Similar procedure was adopted for all the other cycles. The values of the secant stiffness obtained for each cycle are plotted for all the specimens, and the plots are given in Figure 8. It may be noted from this figure that as the number of cycles increases, stiffness decreases. It may also be noted from this figure that the addition of steel fibres to HPC does not have any effect on the first cycle. However, as the number of cycles increases, the rate of degradation of stiffness decreases in the case of HPC specimens additionally reinforced with fibres. The above behaviour may be attributed to the fact that at the first cycle, micro-

cracks would not have initiated and hence the fibres were not effective in the absence of formation of cracks. As the number of cycles increases, micro-cracks develop, and fibres, which are distributed at random, intercept these cracks and bridge across these cracks. This action will control further propagation of cracks and will result in higher energy demand for debonding and pull-out of fibres in the vicinity of cracks. During this process, stiffness of the joint with fibres will not undergo much reduction when compared to that without fibres.

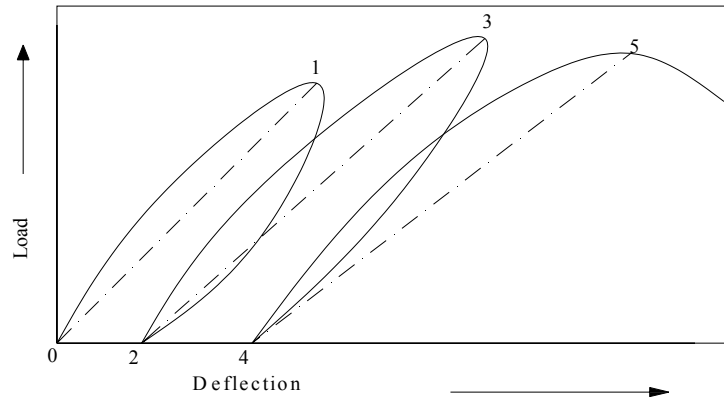


Fig. 7 The procedure adopted for determining secant stiffness

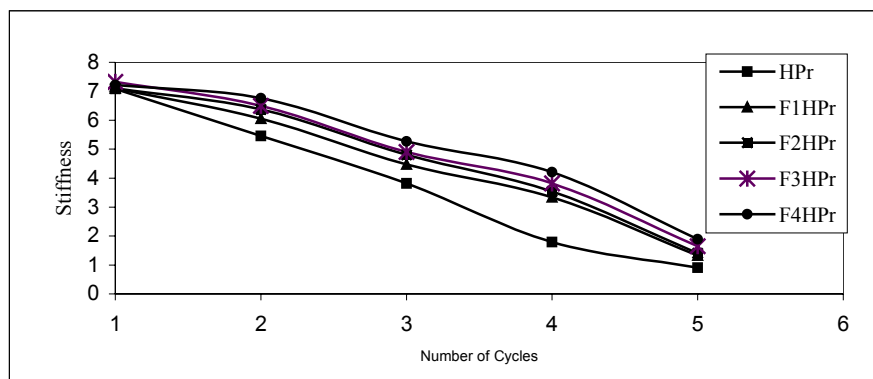


Fig. 8 Relationship between stiffness and number of cycles

SHEAR STRENGTH OF THE JOINT

An attempt has been made to predict shear strength of joints using the following models available in literature for the normal strength concrete. The details of these models are presented elsewhere (Tsonos et al., 1992; Bakir, 2003; Jiuru et al., 1992).

1. Tsonos et al. (1992)

Based on a large number of experimental investigations, Tsonos et al. (1992) suggested a model based on the strut-and-tie concept. The equation for predicting the joint shear strength is as follows:

$$\left[\frac{\alpha\gamma}{2\sqrt{f_c}} \left(1 + \sqrt{1 + \frac{4}{\alpha^2}} \right) \right]^5 + \frac{5\alpha\gamma}{\sqrt{f_c}} \left(\sqrt{1 + \frac{4}{\alpha^2}} - 1 \right) = 1 \quad (2)$$

This equation was developed based on the assumption that both strut and truss mechanisms depend on the core concrete strength.

2. Bakir (2003)

After studying the influence of all possible variables, Bakir (2003) carried out a regression analysis on the test data available in literature. Best regression statistics were obtained by using variables such as

stirrup ratio, stirrup yield strength, concrete cylinder strength, and ratio of height of column to the diameter of beam bars. Effect of the crossed inclined bars provided in the study was also included. Based on these studies, following equation for the joint shear strength was obtained:

$$V = \left(\frac{b_c + b_b}{2} \right) h_c \lambda \left(0.092 f'_c + 0.55 \ln \left(\frac{h_c}{d_b} \right) + 0.23 \frac{A_{sh} f_{ys}}{\left(\frac{b_b + b_c}{2} \right) h_c} \right) \quad (3)$$

3. Jiuru et al. (1992)

A model for predicting the ultimate shear strength of the fibre reinforced joints was developed based on the assumption that even after cracking, considerable tensile stress remains in the concrete until the fibres are pulled out from the matrix. Accordingly the ultimate shear strength is given by

$$V = V_c + V_f + V_s \quad (4)$$

where V_c is the shear carried by the concrete, V_f is the shear carried by the fibres, and V_s is the shear carried by the joint stirrups. These are expressed as

$$V_c = 0.1 \left(1 + \frac{N}{b_c h_c f_{ac}} \right) b_j h_j f_{ac} \quad (5)$$

$$V_f = 2 \frac{l_f}{d_f} v_f b_j h_j \quad (6)$$

$$V_s = f_{ys} \frac{A_{sh}}{S} (d - a'_s) \quad (7)$$

4. Comparison of Analytical Models with Experimental Results

The values of ultimate shear strength computed using the above equations are compared with the experimental values. Details of comparison are given in Table 3. It may be noted from the table that average of the ratio of $V_{(exp.)}$ to $V_{(th.)}$ is 0.86 in the case of Tsonos et al. (1992), 1.48 in the case of Bakir (2003), and 1.74 in the case of Jiuru et al. (1992). This indicates that the comparison is not satisfactory. This may be due to the following reasons. The equations considered in the comparison are meant for either normal concrete, as in the cases of Tsonos et al. (1992) and Bakir (2003), or for fibre reinforced normal concrete, as in the case of Jiuru et al. (1992). Thus, in these equations either the effect of steel fibres or the effect of HPC was not included.

Table 3: Comparison of Ultimate Shear Strength

Specimen	$V_{(exp.)}$ (N/mm ²) (1)	Calculated Values $V_{(th.)}$ (N/mm ²)			Ratio (1)/(2)	Ratio (1)/(3)	Ratio (1)/(4)
		Tsonos*	Bakir**	Jiuru***			
		(2)	(3)	(4)			
HP _r	7.88	12.57	7.28	5.53	0.63	1.08	1.43
HP _r	7.58	12.41	7.22	5.47	0.61	1.05	1.38
F1HP _r	10.45	12.48	7.25	5.83	0.84	1.44	1.79
F1HP _r	9.65	12.62	7.29	5.86	0.76	1.32	1.64
F2HP _r	11.69	12.73	7.36	6.25	0.92	1.59	1.87

F2HP _r	10.21	12.66	7.32	6.22	0.81	1.40	1.64
F3HP _r	12.52	12.99	7.50	6.70	0.96	1.67	1.87
F3HP _r	13.05	13.15	7.53	6.72	0.99	1.73	1.94
F4HP _r	13.24	13.27	7.60	7.11	1.00	1.74	1.86
F4HP _r	13.43	12.93	7.45	6.99	1.04	1.80	1.92
Average					0.86	1.48	1.74
Coefficient of Variation					0.17	0.17	0.12

* Tsonos et al. (1992); ** Bakir (2003); *** Jiuru et al. (1992)

5. Modification Proposed

An attempt has been made to modify the model proposed by Jiuru et al. (1992). In order to account for the effect of HPC in the model, a regression analysis was carried out. A parameter F was introduced to account for the combined effect of steel fibres, compressive strength of concrete, and modulus of rupture, and is given by

$$F = \frac{l_f}{d_f} v_f b_f \frac{f_c'}{f_{cr}} \tag{8}$$

This parameter was related to $V_{(exp.)}/V_{(th.)}$, where $V_{(th.)}$ is given by Equation (4), and the plot is shown in Figure 9. By conducting regression analysis, the modified equation obtained is

$$V_{(exp.)} = V_{(th.)} (0.075F + 1.6284) \tag{9}$$

By replacing $V_{(exp.)}$ by $V_{(pre.)}$, where $V_{(pre.)}$ indicates the predicted shear strength value, the predicted value of shear strength is given by

$$V_{(pre.)} = V_{(th.)} (0.075F + 1.6284) \tag{10}$$

Figure 10 shows the comparison between the predicted and experimental values of ultimate shear strength. All the points are close to the line of equality and lie within $\pm 15\%$ lines of agreement. Hence, the proposed model predicts the shear strength satisfactorily. The proposed model is however only a preliminary model that needs to be improved further with the help of a larger database.

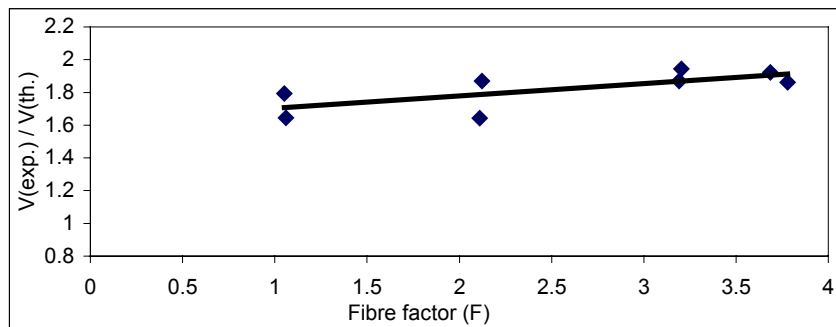


Fig. 9 Relationship between $V_{(exp.)}$ and $V_{(th.)}$ and fibre factor F

CONCLUSIONS

- The SFRHPC joints undergo large displacements without developing wider cracks when compared to the HPC joints. This indicates that steel fibres impart high ductility to the SFRHPC joints, which is one of the essential properties for the beam-column joints.

- Addition of fibres to the beam-column joints decreased the rate of stiffness degradation appreciably when compared to the joints without fibres. Hence, the technique of inclusion of steel fibres in beam-column joints appears to be a useful solution in the case of joints subjected to repeated or cyclic loading.
- During testing it has been noted that addition of fibres could improve the dimensional stability and integrity of the joints.
- Also, it is possible to reduce the congestion of steel reinforcement in the beam-column joints by replacing part of ties in the columns by steel fibres.
- Load carrying capacity of the joints also increased with the increasing fibre content.

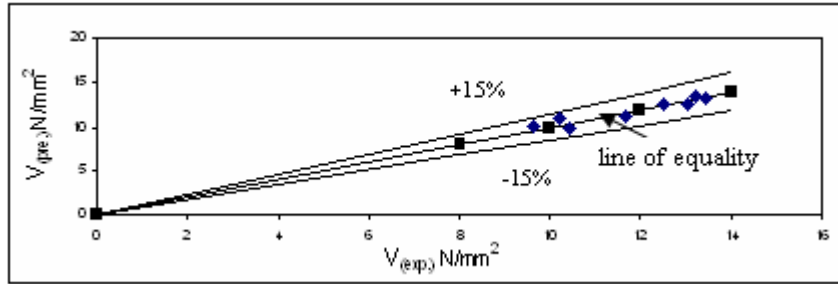


Fig. 10 Comparison between $V_{(exp.)}$ and $V_{(pre.)}$

ACKNOWLEDGEMENTS

This experimental investigation is part of (i) the research project, ‘High Performance Steel Fibre Reinforced Concrete’, funded by MHRD, Government of India, and (ii) the project, “Strength and Ductility of High Performance Concrete Flexural Members Subjected to Seismic Forces”, funded by Kerala State Council for Science Technology and Environment, Government of Kerala. Financial support rendered by them is thankfully acknowledged.

NOTATIONS

- a'_s = distance from extreme compressive fibre to the centroid of compressive reinforcement
 A_{sh} = area of shear reinforcement in the joint
 b_b = width of beam
 b_c = width of column
 b_f = bond efficiency factor (= 0.75)
 b_j = effective width of joint transverse to the direction of shear
 d = effective depth of beam
 d_b = diameter of beam longitudinal reinforcement
 d_f = diameter of fibre
 E_s = modulus of elasticity of steel
 f_{ac} = axial compressive strength of concrete
 f_c = increased joint compressive strength due to confinement ($= Kf'_c$)
 f'_c = compressive strength of concrete

f_{cr}	=	modulus of rupture of concrete
f_{ys}	=	yield strength of transverse reinforcement
h_b	=	total depth of beam
h_c	=	total depth of column
h_j	=	effective depth of joint parallel to the direction of shear
K	=	$1 + \rho_s f_{ys} / f'_c$
l_f	=	length of fibre
N	=	axial compressive load of column
S	=	spacing of stirrups
$V_{(exp.)}$	=	experimental value of ultimate shear strength
$V_{(pre.)}$	=	predicted value of ultimate shear strength
$V_{(th.)}$	=	theoretical value of ultimate shear strength
v_f	=	volume fraction of fibres
x	=	neutral axis depth
ρ_s	=	volume ratio of transverse hoop reinforcement
f_y	=	yield strength of reinforcement
α	=	h_b / h_c
γ	=	joint shear stress expressed as a multiple of $\sqrt{f'_c}$
λ	=	capacity reduction factor (= 0.78)
ϕ_u	=	curvature at ultimate load
ϕ_y	=	curvature at yield load

REFERENCES

1. ACI (1988). "Design Considerations for Steel Fiber Reinforced Concrete", Report 544.4R-88, American Concrete Institute, Farmington Hills, U.S.A.
2. ACI (1998). "Standard Practice for Selecting Proportions for Structural Lightweight Concrete", Report 211.2-98, American Concrete Institute, Farmington Hills, U.S.A.
3. ACI (2002). "Recommendations for Design of Beam-Column Connections in Monolithic Reinforced Concrete Structures", Report 352R-02, American Concrete Institute, Farmington Hills, U.S.A.
4. Aïtcin, P.-C. (1998). "High Performance Concrete", E & FN Spon, London, U.K.
5. Bakir, P.G. (2003). "Seismic Resistance and Mechanical Behaviour of Exterior Beam-Column Joints with Crossed Inclined Bars", Structural Engineering & Mechanics, Vol. 16, No. 4, pp. 493–517.
6. Bayasi, Z. and Gebman, M. (2002). "Reduction of Lateral Reinforcement in Seismic Beam-Column Connection via Application of Steel Fibers", ACI Structural Journal, Vol. 99, No. 6, pp. 772–780.
7. BIS (1989). "IS 8112-1989: Indian Standard 43 Grade Ordinary Portland Cement—Specification (First Revision)", Bureau of Indian Standards, New Delhi.
8. Espion, B. (1994). "Discussion: Flexural Analysis of Reinforced Concrete Beams Containing Steel Fibres", Journal of Structural Engineering, ASCE, Vol. 120, No. 6, pp. 1932–1934.
9. Filiatrault, A., Ladicani, K. and Massicotte, B. (1994). "Seismic Performance of Code-Designed Fibre Reinforced Concrete Joints", ACI Structural Journal, Vol. 91, No. 5, pp. 564–571.

10. Ganesan, N. and Indira, P.V. (2000). "Latex Modified SFRC Beam-Column Joints Subjected to Cyclic Loading", *The Indian Concrete Journal*, Vol. 74, No. 7, pp. 416-420.
11. Gefken, P.R. and Ramey, M.R. (1989). "Increased Joint Hoop Spacing in Type 2 Seismic Joints Using Fibre Reinforced Concrete", *ACI Structural Journal*, Vol. 86, No. 2, pp. 168-172.
12. Jiuru, T., Chaobin, H., Kaijian, Y. and Yongcheng, Y. (1992). "Seismic Behaviour and Shear Strength of Framed Joint Using Steel-Fiber Reinforced Concrete", *Journal of Structural Engineering, ASCE*, Vol. 118, No. 2, pp. 341-358.
13. Kumar, V., Nautiyalil, B.D. and Kumar, S. (1991). "A Study of Exterior Beam-Column Joints", *The Indian Concrete Journal*, Vol. 65, No. 1, pp. 39-43.
14. Oh, B.H. (1992). "Flexural Analysis of Reinforced Concrete Beams Containing Steel Fibres", *Journal of Structural Engineering, ASCE*, Vol. 118, No. 10, pp. 2821-2836.
15. Shamim, M. and Kumar, V. (1999). "Behaviour of Reinforced Concrete Beam-Column Joint—A Review", *Journal of Structural Engineering, ASCE*, Vol. 26, No. 3, pp. 207-213.
16. Shannag, M.J., Abu-Dyaa, N. and Abu-Farsakh, G. (2005). "Lateral Load Response of High Performance Fiber Reinforced Concrete Beam-Column Joints", *Construction and Building Materials*, Vol. 19, No. 7, pp. 500-508.
17. Soubra, K.S., Wight, J.K. and Naaman, A.E. (1993). "Cyclic Response of Cast-in-Place Connections in Precast Beam-Column Subassemblages", *ACI Structural Journal*, Vol. 90, No. 3, pp. 316-323.
18. Tsonos, A.G., Tegos, I.A. and Penelis, G.G. (1992). "Seismic Resistance of Type 2 Exterior Beam-Column Joints Reinforced with Inclined Bars", *ACI Structural Journal*, Vol. 89, No. 1, pp. 3-12.